

Statistical picture of high energy nuclear collisions

Jörn Knoll

*Max-Planck-Institut für Kernphysik, D-6900 Heidelberg, Germany
and Institute for Nuclear Study, University of Tokyo, Tokyo 188, Japan*

(Received 29 December 1978)

We discuss nuclear reactions induced by nucleons or heavy ions at incident energies in the range of 0.5 to 1 GeV/nucleon. One-particle spectra and the correlations of two nucleons emitted are studied in the statistical limit: Subgroups of nucleons acquire a random occupation of their available phase space. As opposed to the thermal limit the finite number of nucleons gives rise to sizable correlations among the nucleons via the conservation laws. A surprising reproduction of the observed spectra—in particular at high momentum transfers (as in proton backward scattering)—is achieved by the model.

NUCLEAR REACTIONS Proton and heavy ion induced; $E = 0.5\text{--}1.0$ GeV/nucleon; calculation of inclusive one- and two-proton (coincidence) spectra by statistical model.

I. INTRODUCTION

A great variety of theoretical models¹⁻¹⁰ have been equally successful in describing the gross features of proton inclusive spectra resulting from high-energy nuclear collisions.^{1,11} They range from the most simple thermal-limit models¹⁻² through simplified multiple collision pictures³⁻⁷ to sophisticated full scale intranuclear cascade, hydrodynamical and classical dynamics models.⁸⁻¹⁰ The study of the thermalization hypothesis suggested by the relative success of the thermal models was one of the major objectives of the simplified multiple collision model.⁴ The analysis which has recently been extended to the energy domain above the Δ isobar threshold⁶ draws attention to a relatively fast equilibration within subgroups of nucleons with respect to various observables. On the other hand, the recently observed correlations between two ejected protons¹¹ are beyond the scope of any thermal model.

It is the aim of this note to present a study which, in its major ingredients, is as simple as the thermal models: The central idea is that each nucleon undergoes only a limited number of collisions with other nucleons. That is to say well confined groups of nucleons interact with each other. Their final momentum distributions are assumed to follow from the random occupation of the available phase space. Through the conservation laws these distributions imply a considerable correlation among the nucleons, as their number is small. The initial Fermi motion is included by an appropriate folding procedure.

The present study does not aim at fitting data. Rather we consider it as a background approach which, in the event of agreement with the data, draws attention to those situations where major

dynamical effects remain masked. This might be due to either the lack of more observed information or processes where in fact a large number of interactions lead towards equilibration.

II. THE GENERAL DESCRIPTION OF INCLUSIVE SPECTRA

Before we start to explain the details of the model we wish to introduce a general frame for the description of such reactions.

For simplicity we first concentrate on the reaction of a nucleon with a nucleus A . We classify the various events by the number N of (target) nucleons which interact with the beam nucleon. This picture coincides with the exciton model¹² where the incident nucleon creates an N -particle- N -hole excitation. Therefore, both the one- and the two-particle cross sections arise from an incoherent sum over the different processes

$$\begin{aligned} \epsilon \frac{d^3\sigma}{d^3p} &= \sum_N \sigma_A(N) F_{IN}^1(\vec{p}), \\ \epsilon\epsilon' \frac{d^6\sigma}{d^3p d^3p'} &= \sum_N \sigma_A(N) F_{IN}^2(\vec{p}, \vec{p}'). \end{aligned} \quad (1)$$

Here ϵ , \vec{p} and ϵ' , \vec{p}' denote the respective energies and momenta of the observed particles. We have purposely extracted the cross sections $\sigma_A(N)$ (hereafter called section areas) of these different processes. The spectral output of the reaction is contained in the appropriately normalized [cf. Eq. (4)] one- and two-particle distributions F .

The picture changes in going over to nucleus-nucleus collisions. Here it is possible that simultaneously in a single event different groups of nucleons contribute to the resulting spectra. We label each such group of interacting nucleons by the numbers M and N of its projectile and target

members. Through the assumption that the different contributing groups behave independently, the corresponding one-particle spectrum results from an incoherent sum similar to (1),

$$\epsilon \frac{d^3\sigma}{d^3p} = \sum_{MN} \sigma_{AB}(M, N) F_{MN}^1(\vec{p}). \quad (2)$$

Now $\sigma_{AB}(MN)$ defines the cross section that the respective subprocess has in the collision of the nuclei A and B . We omit the contributions of those nucleons which have not encountered a single interaction. The contributions of these spectators dominate the fragmentation cross section¹³ which we do not consider here. We note that the two-particle cross section arises from two terms: a correlated one where the observed pair of nucleons results from the same group M, N and, if different groups are the source, an uncorrelated background term,

$$\begin{aligned} \epsilon \epsilon' \frac{d^6\sigma}{d^3p d^3p'} &= \sum_{MN} \sigma_{AB}(M, N) [F_{MN}^2(\vec{p}, \vec{p}') \\ &\quad - F_{MN}^1(\vec{p}) F_{MN}^1(\vec{p}')] \\ &\quad + \sum_{MNM'N'} \sigma_{AB}(M, N; M', N') F_{MN}^1(\vec{p}) F_{M'N'}^1(\vec{p}'). \end{aligned} \quad (3)$$

The spectral functions are normalized to the number of nucleons and pairs, respectively,

$$\begin{aligned} \int \frac{d^3p}{\epsilon} F_{MN}^1(\vec{p}) &= M + N, \\ \int \frac{d^3p}{\epsilon} \frac{d^3p'}{\epsilon'} F_{MN}^2(\vec{p}, \vec{p}') &= (M + N)(M + N - 1). \end{aligned} \quad (4)$$

One of the main reasons for the particular separation into *section areas* and appropriately normalized *spectral functions* F is the following. One can already obtain a fair estimate of the section areas from particular sum rules. These relate the section areas to experimental observables in the form of the reaction cross sections and the moments of the respective *nucleon* multiplicity distributions $\langle \nu^k \rangle$.¹⁴ For the nucleon-nucleus collision one finds (cf.¹⁵)

$$\begin{aligned} \sum_N \sigma_A(N) &= \sigma_A, \\ \sum_N (N+1)^k \sigma_A(N) &= \sigma_A \langle \nu^k \rangle_{1A}. \end{aligned} \quad (5)$$

Since we omit the spectator contributions, there are fewer relations in the nucleus-nucleus case

$$\begin{aligned} \sum_{MN} (M+N) \sigma_{AB}(M, N) &= \sigma_{AB} \langle \nu \rangle_{AB}, \\ \sum_{MNM'N'} (M+N)(M'+N') \sigma_{AB}(M, N; M', N') &= \sigma_{AB} \langle \nu^2 \rangle_{AB}. \end{aligned} \quad (6)$$

Here $\sigma_{AB} \approx \pi(R_A + R_B)^2$ is the corresponding reaction cross section.

The scheme developed above¹⁻⁶ is fairly general. It encompasses practically all multiple collision models. In principle—apart from the spectral distributions F —the section areas are also an involved consequence of the complicated many-body dynamics. They may equally include either a trumpetlike opening of the participant matter or a possible premature escape of a nucleon at the surface.

It is through various, generally simplifying, assumptions upon both the section areas and the spectral output that different models emerge. The high-energy Glauber picture as employed below helps in deriving simple estimates of the section areas. The restriction to the knock-out limit³ of quasifree scattering is as obvious as the thermal-limit picture. The dynamical linear-cascade model⁴ provides a continuous link between the above extremes. It constructs the distributions F through a sequence of binary collisions. Its two-particle correlation part has recently been studied by a Monte Carlo simulation method.¹⁶

III. THE MODEL

We will specify the simplifications adopted in the present study. According to the frame developed above two ingredients are incorporated: (i) the section areas which in the present picture merely reflect the initial geometry of the nuclei and (ii) the spectral distributions which contain the dynamical aspects of the processes.

A. The geometry

We borrow the recipe for calculating the section areas from the high-energy Glauber picture of straight-line motion.^{17, 4-7} There, the section areas result from an impact parameter integrated Poisson distribution

$$\begin{aligned} \sigma_A(N) &= \int d^2s P_A(N, \vec{s}), \\ P_A(N, \vec{s}) &= \frac{1}{N!} [\bar{N}_A(\vec{s})]^N \exp[-\bar{N}_A(\vec{s})]. \end{aligned} \quad (7)$$

The mean number $\bar{N}_A(\vec{s})$ is given by the matter $\rho_A(\vec{r})$ compiled in the beam direction within an area of the total NN cross section σ_{NN}^{tot} ,

$$\bar{N}_A(\vec{s}) = \sigma_{NN}^{\text{tot}} \int_{-\infty}^{\infty} \rho_A(\vec{s}, z) dz. \quad (8)$$

Transcribing the straight-line idea to the nucleus-nucleus case gives a factorized form

$$\sigma_{AB}(M, N) = \sigma_A(M) \sigma_B(N) / \sigma_{NN}^{\text{tot}}. \quad (9)$$

It implies the geometrical sum-rule result

$$\langle \nu \rangle_{AB} \sigma_{AB} = \int d^3p \frac{d^3\sigma}{d^3p} = A\sigma_B + B\sigma_A, \quad (10)$$

where

$$\sigma_{AB}(M, N; M', N') = \int d^2b \frac{d^2s_A d^2s_B}{\sigma_{NN}^{\text{tot}}} \frac{d^2s'_A d^2s'_B}{\sigma_{NN}^{\text{tot}}} \delta^2(\vec{s}_A - \vec{s}_B - \vec{b}) \delta^2(\vec{s}'_A - \vec{s}'_B - \vec{b}) P_A(M, \vec{s}_A) P_B(N, \vec{s}_B) P_A(M', \vec{s}'_A) P_B(N', \vec{s}'_B). \quad (12)$$

Here the two δ functions ensure that both combinations occur at the same impact parameter \vec{b} .

We use the same specifications as in Ref. 6, where we chose $\sigma_{NN}^{\text{tot}} = 40$ mb and a standard Woods-Saxon form for the matter densities. Further details about the sections areas are explained there, too.

We like to clarify that in adopting the straight-line approximation we do not pretend that the process actually evolves in a collinear way. Rather, the lack of more refined expressions compels us to take them as an appropriate guess.

B. The statistical limit

The spectral distribution resulting from a collision of a group of $k = M + N$ nucleons can be written in the general form (the upper label refers to the number of observed particles)

$$F_{MN}^k(\vec{p}_1, \dots, \vec{p}_k) = \bar{S}_{MN}^k(\vec{p}_1, \dots, \vec{p}_k) \phi_k^k(\vec{p}_1, \dots, \vec{p}_k), \quad (13)$$

where \bar{S} contains the dynamical information of the process $\{MN\}$ and the *phase space function* ϕ ensures the kinematical conservation laws. In the event of precisely given initial total energy E_{MN} and momentum P_{MN} the latter is

$$\phi_k^k(\vec{p}_1, \dots, \vec{p}_k) = \delta^3\left(\vec{P}_{MN} - \sum_{i=1}^k \vec{p}_i\right) \delta\left(E_{MN} - \sum_{i=1}^k \epsilon_i\right) / I_k(s), \quad (14)$$

with the square of the invariant mass

$$s = E_{MN}^2 - P_{MN}^2.$$

This corresponds to a microcanonical ensemble with an isotropic occupation of the energy shell in the $3k$ -dimensional momentum space. The phase space integral $I_k(s)$ normalizes the distribution ϕ to one.

As already mentioned, the function \bar{S}_{MN} contains the dynamical information of the process $\{MN\}$. In a rigorous theory it would be constructed by the square of the corresponding cluster part of

$$\sigma_A = \int d^2s \{1 - \exp[-\bar{N}_A(\vec{s})]\}. \quad (11)$$

The section areas for finding simultaneously two groups of interacting nucleons are found to be

the S matrix summed over all final states which are in line with the momenta specified in (13); in a diagrammatic picture this would correspond to all diagrams which contain a connected piece of precisely M projectile and N target lines. In the simple case of elastic two-body scattering ($M = N = 1$), the dynamical structure function would be proportional to the elastic differential cross section

$$\bar{S}_{11}^2(\vec{p}_1, \vec{p}_2) = \frac{8\pi}{\sigma_{NN}^{\text{tot}}} \frac{d\sigma(\theta_{\text{c.m.}})}{d\Omega}, \quad (15)$$

where $\theta_{\text{c.m.}}(\vec{p}_1, \vec{p}_2)$ is the respective c.m. scattering angle. A factor of two arises because of the normalization (4).

In actual measurements only a few particles out of the considered cluster are observed. The corresponding spectral function which results from (13) by integrating over the unobserved particles can be written in a similar form

$$F_{MN}^L(\vec{p}_1, \dots, \vec{p}_L) = \bar{S}_{MN}^L(\vec{p}_1, \dots, \vec{p}_L) \phi_k^L(\vec{p}_1, \dots, \vec{p}_L), \quad (16)$$

where now ϕ_k^L is the probability distribution of the L observed momenta of the *random ensemble* (14). Thus

$$\phi_k^L(\vec{p}_1, \dots, \vec{p}_L) = \int \frac{d^3p_{L+1}}{\epsilon_{L+1}} \dots \frac{d^3p_k}{\epsilon_k} \phi_k^k(\vec{p}_1, \dots, \vec{p}_k). \quad (17)$$

The statistical limit as invented by Fermi¹⁸ (see also Hagedorn¹⁹) assumes that the particular dynamics of the process has only gentle implications on the observed spectrum. That is to say, the spectral function is dominated by the behavior of the phase space distributions. Intuitively, this appears to be more justified as the number of observed particles is considerably smaller than the size of the ensemble, or in other words as the phase space which covers the unobserved information is sufficiently large. In the present approach we adopt the strict limit of least dynamical information which means $\bar{S}_{MN} = \text{const.}$ It

corresponds to the random limit where each result compatible with the conservation laws is as probable as another. This picture deviates from the phase space limit of the exciton model¹² where the momentum conservation is completely ignored.

The phase space distributions are known to have the explicit solutions for

$$\phi_k^L(\vec{p}_1, \dots, \vec{p}_L) = I_{k-L} \left[\left(E_{MN} - \sum_{i=1}^L \epsilon_i \right)^2 - \left(\vec{P}_{MN} - \sum_{i=1}^L \vec{p}_i \right)^2 \right] / I_k(s), \quad (18)$$

where the phase space integrals can be constructed recursively²⁰

$$I_{k+1}(s) = \frac{\pi}{s} \int_{s_1}^{s_2} ds' (\lambda(s, s', m^2))^{1/2} I_k(s),$$

$$\lambda(x, y, z) = x^2 + y^2 + z^2 - 2xy - 2xz - 2yz,$$

$$s_1 = k^2 m^2, \quad s_2 = (\sqrt{s} - m)^2, \quad (19)$$

$$I_1(s) = 2\delta(s - m^2).$$

For illustration we discuss the one-particle spectrum ϕ_k^1 . It is an isotropic function in the respective center of momentum frame. As the size of the ensemble grows this distribution is expected to approach the thermal limit: The Maxwell Boltzmann distribution. This is illustrated in Fig. 1. Ensembles with small nucleon number, however, deviate from the thermal limit ($k = \infty$) showing a depression at moderate c.m. momenta and a steeper falloff at the kinematical limit of the phase space. In particular, the two-particle ensemble has a δ -function shape at a c.m. momentum corresponding to the energy conservation. According to (15) it is identical to the isotropic two-body scattering event.

So far we assumed that the considered ensembles $\{MN\}$ have precisely given initial total energy and

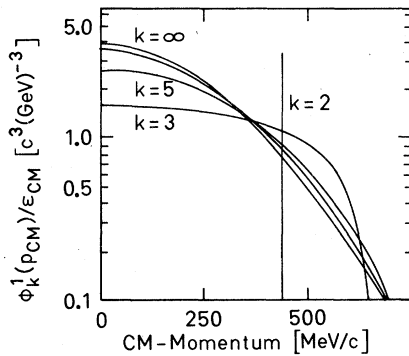


FIG. 1. The one-particle spectrum $\phi_k^1(p_{c.m.})$ as a function of the c.m. momentum of the statistical ensemble of $K=2, 3, 5, 10,$ and ∞ members. The c.m. energy per particle is 100 MeV. The spike indicates the position of the δ function of the $K=2$ ensemble.

momentum. This is in fact not the case because of the Fermi motion. This leads to a finite width of the knockout ($M=N=1$) distributions and to essential corrections at the kinematical limits of each ensemble. We include these effects by a folding over the respective Fermi momentum distributions

$$F_{MN}^L(p_1, \dots, p_L) = \frac{k!}{(k-L)!} \int d^3P_A d^3P_B \omega_M(\vec{P}_A) \omega_N(\vec{P}_B) \times \phi_k^L(p_1, \dots, p_L; E_{MN}, \vec{P}_{MN}). \quad (20)$$

Neglecting the binding energies of the nucleons, the lab energy and momentum components parallel and perpendicular to the beam are

$$E_{MN} = M(E_0 + P_0 P_{A||}/m) + Nm,$$

$$P_{MN||} = M(P_0 + E_0 P_{A||}/m) + NP_{B||}, \quad (21)$$

$$P_{MN\perp} = MP_{A\perp} + NP_{B\perp}.$$

The Fermi momentum distribution of the total momentum \vec{P}_A of the M nucleons of nucleus A (similarly for B) with respect to its rest frame are assumed to be Gaussian

$$\omega_M(P_A) = [2\pi\sigma_{AM}^2]^{-3/2} \exp(-\frac{1}{2}P_A^2/\sigma_{AM}^2). \quad (22)$$

The independent particle model prescription for the width²¹ gives

$$\sigma_{AM}^2 = \frac{M(A-M)}{A-1} \frac{1}{5} k_{FA}^2, \quad (23)$$

where k_{FA} is the respective Fermi momentum.

The folding procedure (20) is calculated by the corresponding multidimensional saddle point method. The calculations are performed with a Fermi momentum of 230 MeV/c for carbon and 260 MeV/c for all heavier nuclei.

IV. APPLICATIONS AND DISCUSSIONS

The present model rests on two basis assumptions: (i) Each event is thought to be built up by uncorrelated contributions arising from the interaction of different *subgroups* of nucleons. Their relative weights are estimated from the geometrical concept of straight lines. (ii) the corresponding momentum distributions are constructed from the statistical limit where the nucleons of each group *randomly* explore the available phase space. The initial Fermi motion is included by a folding procedure. The model represents the ultimate limit of any multiple collision picture: the limit of many collisions. This limit will be viewed in conjunction with the opposite extreme: the knockout picture, where each nucleon undergoes a single quasifree scattering at most.

Exploratory calculations have been performed with the present model. The selected examples

illustrate those features of the spectra which are characteristic for this approach.

We start the discussion with the type of reactions where the best agreement with data is achieved.

These are the proton spectra resulting from high-energy nucleus-nucleus collisions, Fig. 2. The agreement is not only limited to the bulk part of the spectrum but rather—besides a slight overestimation there—persists even up to the high momentum extremes of the spectrum (a “cooling” induced through the inclusion of pionic degrees of freedom might even help improving the agreement). The main contributions in our picture come from terms with $M \approx N \approx 3$ where—to say—each nucleon has undergone about three collisions.

As the spectra of systems with equal projectile and target mass with their nonisotropic shapes in the c.m. frame rule out a complete equilibration of *all* participants (fireball) they confirm one of our assumptions: Equilibria—if at all—establish themselves only among well confirmed subgroups of the participating nucleons.

Correlation measurements are even more sensitive on this partition into subgroups of interacting nucleons. They were proposed for a more detailed analysis of the dynamics of heavy-ion collisions. In order to elucidate this point we discuss the recently observed ratio R of the in- to out-of-plane coincidence rate of two protons, Fig. 3. The

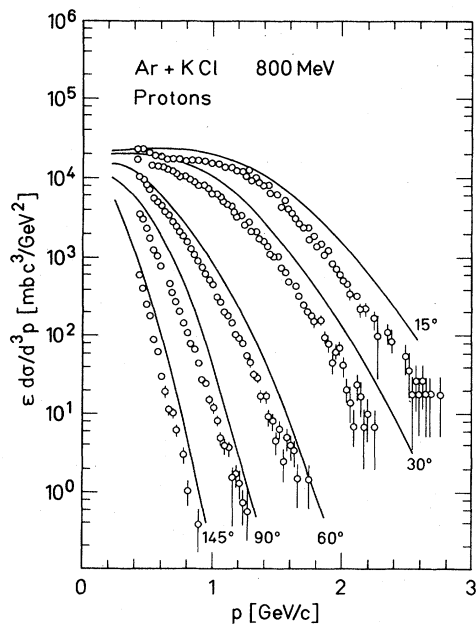


FIG. 2. Proton inclusive spectrum of the reaction $\text{Ar} + \text{KCl} \rightarrow p + X$ at 800 MeV/nucleon for various lab angles as a function of the lab momentum of the observed proton (data from Ref. 11).

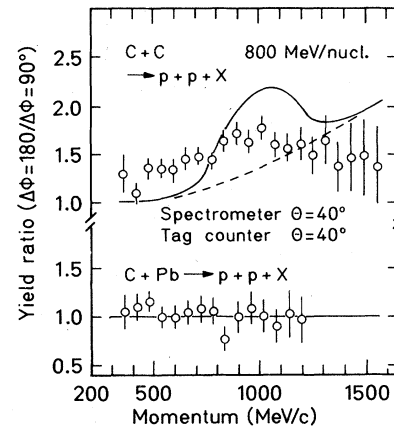


FIG. 3. Coincidence measurement of two protons observed at the same scattering angle $\theta_i = 40^\circ$ and different azimuthal angles φ_i . The ratio R gives the coincidence rate at $\varphi_1 - \varphi_2 = 180^\circ$ (in-plane configuration) relative to the rate at $\varphi_1 - \varphi_2 = 90^\circ$ (out-of-plane configuration) as a function of the momentum P of proton 1. Proton 2 is registered for all energies above 100 MeV. The full line is the result of the present model, the dashed line excludes the knockout $M=N=1$ contributions.

kinematics was chosen such that the symmetric quasifree NN scattering (90° in c.m. frame) can be observed in the in-plane configuration (for details see Ref. 11). The so expected quasifree scattering peak at a momentum of about 1 GeV/c of the spectrometer proton corresponds to the contribution of $M=N=1$. This peak bears the width due to Fermi motion. However, in deviation from the knockout picture³ the present study also predicts a sizable correlation for those groups with more than two nucleons (dashed line). The latter notably raise the ratio at large spectrometer momenta, an aspect which should be clarified by more accurate data. The remaining deviations from the data ask for refined treatments. Part of them can be attributed to two reasons: (i) The anisotropy of the NN cross section causes deviations from the isotropic knockout contributions here considered; and (ii) a sizable production of $\Delta(1236)$ isobars reduces the coincidence rate at the quasifree scattering peak in favor of an enhancement of R at lower momenta. Our studies also show that an additional spectrometrical measurement of the second proton would amplify the correlation effect to a peak value of $R=3.5$ in carbon on carbon.

The following two examples concentrate on high-energy proton-nucleus collisions. Here we focus our attention on the particularly interesting part of the spectrum at high momentum transfer.²² Besides the simplest knockout picture employed

by Amado and Woloshyn²³ where nucleons with fairly high momenta have to be picked up by the reaction, particular mechanisms like the fluctuons picture²⁴ or the correlated cluster model²⁵ have been invented to generate such high momentum transfer. Our aim is to learn from the statistical limit how probable such events are from the perspective of a multiple collision picture.

Surprisingly, we find a rather remarkable agreement with the data (Fig. 4). Besides a systematic overestimation of about a factor of two for *all targets* and *various incident energies*, the data are nicely followed even up to momentum transfers of 2 GeV/c. Though these calculation sensitively depend on the Fermi momentum chosen, the agreement with the data occurred for the normal value of 260 MeV/c. Thus these results contradict the knockout picture initially employed; namely, they cast some doubts whether the high-momentum component of the nucleon's momentum distribution can be actually studied this way. Rather proceeding in a single step, multiple collision processes seem more likely to generate these high momentum transfer. In our picture the major contribution arises from terms where about four target nucleons are involved. As we learned in addition from a multiple collision approach⁶ that such subprocesses lead to spectra which have already a fairly random appearance, one might even drop the necessity of particular correlations.

The correlated cluster idea was the major motivation for the Dubna $C(p, 2p)$ correlation experiments,²⁶ Fig. 5. Backward emitted protons are registered in the coincidence with a proton in the forward hemisphere. The energy windows are purposely chosen such that the knockout process is kinematically unimportant. This opens the

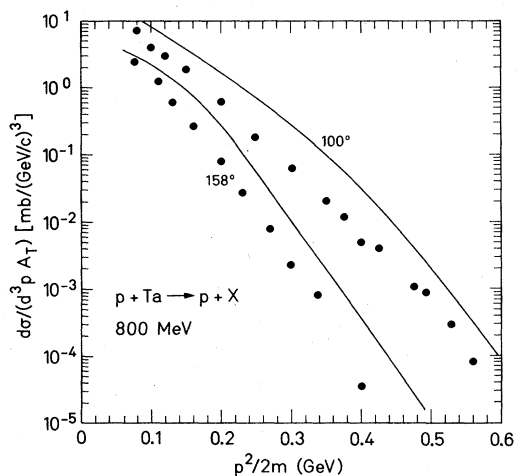


FIG. 4. Backward emitted protons (Ref. 22) in the reaction $p + \text{Ta} \rightarrow p + X$ at 800 MeV.

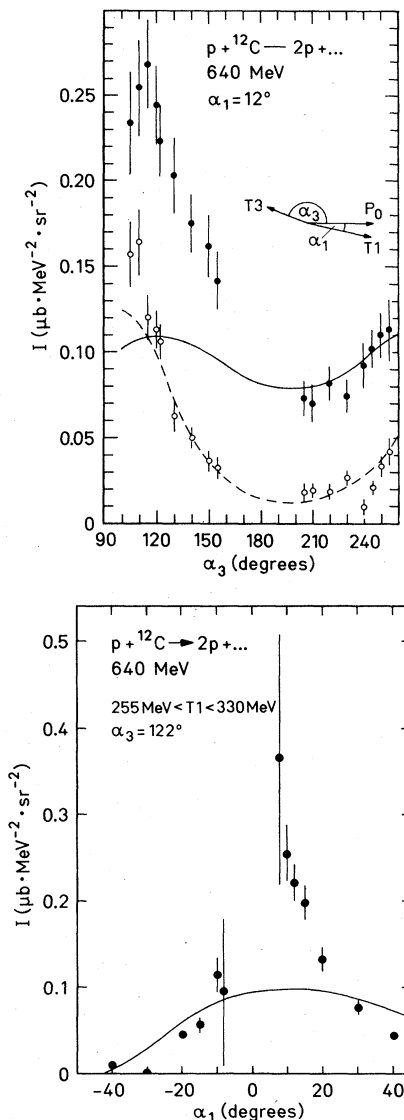


FIG. 5. The coincidence rate of two protons (Ref. 26) at scattering angles α_1 and α_3 as explained in the figure. The open and full data points correspond to a kinetic energy regime of the backward registered proton of $105 \text{ MeV} < T_3 < 150 \text{ MeV}$ and $50 \text{ MeV} < T_3 < 90 \text{ MeV}$, respectively.

analysis for a three-body process. Our model succeeds in reproducing parts of the spectrum. However, it fails in piling up that peak observed at the angle combination of $\alpha_1 = 12^\circ$ and $\alpha_3 = 120^\circ$. This precisely corresponds to the kinematical situation where the presumed unobserved third nucleon has about the same momentum as the forward emitted observed one. As known from three-body dynamics, the long lasting final state interaction of the two parallel moving nucleons causes such deviations from the bare phase space

distribution. Therefore, in this case, our analysis directly draws attention to a *final state correlation* of the emitted nucleons. But even more; as from the kinematical conditions chosen the final state interaction peak only occurs if precisely *three* nucleons are engaged, we encounter [similar to (p, d) reactions] the rare event of isolating a three-body process embedded into a many-body system. Here off-shell effects of the interactions involved may even play an important role for the production of these events.

V. CONCLUSION

We studied spectra of protons emitted in high-energy nuclear reactions from a very simple picture: the statistical limit of a random occupation of the available phase space. Whereas the two-body kinematics employed in the knockout picture required a rather peculiar momentum distribution for the internal motion of nucleons in nuclei^{3,23} for just getting a rough reproduction of the data, our model works with a normal Gaussian shape Fermi distribution. The detailed analysis showed that there are spectra of at least parts of such which can be reproduced by our simple statistical picture. Such instants draw attention to the fact that multiple collision contributions are not negligible and are in fact necessary to understand the data. However, those reactions with spectra which have already a fairly random appearance may be rather weakly predictive about the particular dynamics of the process. Different dynamical theories may lead to similar agreement with data. By far more interesting and decisive are those cases where the present predictions fail to reproduce the data. They focus on particular dynamical effects of var-

ious origins such as pre-equilibrium situations, correlations among nucleons, and final state interactions. Still, the overall agreement of this model with the investigated data clarifies the following: (i) The straight-line estimate of the section areas might not be so seriously in error. They decisively determine the magnitude of the various processes, in particular the correlation parts. (ii) The necessity of multiple collision contribution which in the discussed energy regime may have already a fairly random appearance. (iii) There are effectively no important long range final state interactions which would sensitively destroy the random appearance of the spectra. The last point might be a serious handicap for applying the present consideration to low-energy processes. There, Coulomb forces play a non-negligible role in the final stage of the reaction.

In order to gain a better insight into the development of the discussed reactions forthcoming studies should certainly aim at investigating them by dynamical theories. The linear cascade models^{4,6} as well as the correlation models²⁴⁻²⁵ are already an attempt in that direction. Still, one should not lose sight of the limiting aspect of such theories: the random limit where different dynamical pictures converge indistinguishably.

It is a pleasure to thank T. Fujita, M. Gyulassy, J. Hüfner, H. J. Pirner, J. Randrup, and B. Schürmann for helpful and stimulating discussions. I am indebted to M. Kawai and T. Marumori for their kind hospitality extended to me during my stay in Japan, during which major parts of this work have been pursued. The support of the Japan Society for Promotion of Science is gratefully acknowledged.

¹G. D. Westfall, J. Gosset, P. J. Johanson, A. M. Poskanzer, W. G. Meyer, H. H. Gutbrod, A. Sandoval, and R. Stock, *Phys. Rev. Lett.* **37**, 1202 (1976); J. Gosset, H. H. Gutbrod, W. G. Meyer, A. M. Poskanzer, A. Sandoval, R. Stock, and G. D. Westfall, *Phys. Rev. C* **16**, 629 (1977).
²W. D. Myers, *Nucl. Phys.* **A296**, 177 (1978).
³S. E. Koonin, *Phys. Rev. Lett.* **39**, 680 (1977).
⁴J. Hüfner and J. Knoll, *Nucl. Phys.* **A290**, 460 (1977).
⁵J. Randrup, *Phys. Lett.* **76B**, 547 (1978).
⁶J. Knoll and J. Randrup, *Nucl. Phys. A* (to be published).
⁷H. J. Pirner and B. Schürmann, *Nucl. Phys.* **A316**, 461 (1979).
⁸A. Amsden, J. N. Ginocchio, F. H. Harlow, J. R. Nix, M. Danos, E. C. Halbert, and R. K. Smith, *Phys. Rev. Lett.* **38**, 1055 (1977).
⁹J. P. Bondorf, P. J. Siemens, S. Garpman, and E. Halbert, *Z. Phys.* **279**, 385 (1976).
¹⁰A. R. Bodmer and C. N. Panos, *Phys. Rev. C* **15**, 1342 (1977).

¹¹S. Nagamiya, I. Tanihata, S. Schnetzer, L. Anderson, W. Brückner, O. Chamberlain, G. Shapiro, and H. Steiner, in *Proceedings of the International Conference on Nuclear Structure, Tokyo, 1977*, edited by T. Marumori (Physical Society of Japan, Tokyo, 1978); *J. Phys. Soc. Jpn.* **44**, Suppl. 378 (1978); S. Nagamiya, L. Anderson, W. Brückner, O. Chamberlain, M.-C. Lemaire, S. Schnetzer, G. Shapiro, H. Steiner, and I. Tanihata, *Phys. Lett.* **81B**, 147 (1979).
¹²J. J. Griffin, *Phys. Rev. Lett.* **17**, 478 (1966); M. Blann, *Annu. Rev. Nucl. Sci.* **25**, 123 (1975).
¹³A. S. Goldhaber and H. H. Heckmann, *Annu. Rev. Nucl. Part. Sci.* **28**, 161 (1978).
¹⁴S. Y. Fung, W. Gorn, G. P. Kiernan, F. F. Liu, J. J. Lu, Y. T. Oh, J. Ozawa, R. T. Poe, L. Schroeder, and H. Steiner, *Phys. Rev. Lett.* **40**, 292 (1978); J. Knoll, J. Hüfner, and A. Bouyssy, *Nucl. Phys.* **A308**, 500 (1978).
¹⁵L. Fou, *Phys. Rep.* **22C**, 1 (1975).
¹⁶J. Randrup, *Nucl. Phys.* **A316**, 509 (1979).

- ¹⁷R. Glauber and G. Mathiae, Nucl. Phys. B21, 135 (1970).
- ¹⁸E. Fermi, Prog. Theor. Phys. 5, 570 (1950).
- ¹⁹R. Hagedorn, *Relativistic Kinematics* (Benjamin, New York, 1963).
- ²⁰J. Knoll, Lecture Notes, Institute for Nuclear Studies, Tokyo, Report No. INS-NUMA-9, 1978 (unpublished).
- ²¹A. S. Goldhaber, Phys. Lett. 53B, 306 (1974).
- ²²S. Frankel, W. Frati, G. Blanpied, G. W. Hoffmann, T. Kozlowski, C. Morris, H. A. Thiessen, O. Van Dyck, and C. Whitten, Phys. Rev. C 18, 1375 (1978).
- ²³R. D. Amado and R. M. Woloshyn, Phys. Rev. Lett. 36, 1435 (1976); S. Frankel, Phys. Rev. Lett. 38, 1338 (1977).
- ²⁴V. V. Burov, V. K. Lukyanov, and A. I. Titov, Phys. Lett. 67B, 46 (1977).
- ²⁵T. Fujita, Phys. Rev. Lett. 39, 174 (1977); and T. Fujita, Nucl. Phys. A (to be published).
- ²⁶V. I. Komarov, G. E. Kosarev, H. Müller, D. Netzbund, T. Stiehler, and S. Tesch, Phys. Lett. 80B, 30 (1979).